Study of Doppler broadening Compton scattering and cross section determination for the elements Fe, Zn, Ag, Au and Hg

Wrood K. Abood, Mahdi H. Jasim

Department of Physics, College of Science, University of Baghdad, Baghdad, Iraq

E-mail: wrood_k@yahoo.com

Abstract

To assess the contribution of Doppler broadening and examine the Compton profile, the Compton energy absorption cross sections are measured and calculated using formulas based on a relativistic impulse approximation. The Compton energy-absorption cross sections are evaluated for different elements (Fe, Zn, Ag, Au and Hg) and for a photon energy range (1 - 100 keV). With using these cross-sections, the Compton component of the mass–energy absorption coefficient was derived, where the electron momentum prior to the scattering event caused a Doppler broadening of the Compton line. Also, the momentum resolution function was evaluated in terms of incident and scattered photon energy and scattering angle. The results of cross sections for the coherent and incoherent processes are compared with theoretical values and reported values of other researchers. The present results are in agreement with the theoretical values.

Key words

Doppler broadening, Compton profile, cross section.

Article info.

Received: Jun. 2015
Accepted: Sep. 2015
Published: Apr. 2016

دراسة توسيع دوبلر لاستطارة كومبتون وتحديد المقاطع العرضية للعناصر Fe, Zn, Ag, Au و Hg

ورود كريم عبود، مهدي هادي جاسم

قسم الفيزياء، كلية العلوم، جامعة بغداد، بغداد، العراق

الخلاصة

لتخمين إسهام توسيع دوبلر واختبار الصورة الجانبية لكومبتون، تم قياس وحساب المقاطع العرضية لامتصاص طاقة كومبتون باستخدام صيغ تستند على نموذج تقريب الاندفاع النسبي. تم حساب المقاطع العرضية لامتصاص طاقة كومبتون ولعدة عناصر (Fe, Zn, Ag, Au و Hg) ولمدى طاقة فوتون بين 1-100ك.أ.ف. وباستخدام هذه المقاطع العرضية اشتقت مركبة كومبتون لمعامل الامتصاص الكتلة - الطاقة، حيث ان زخم الاليكترون قبل حدوث التشتت سبب في ظهور توسع دوبلر في خط كومبتون. كذلك تم ايجاد قيم دالة ميز الزخم بدلالة طاقة الفوتون الساقط والمشتت وزاوية التشتتقورنت نتائج المقاطع العرضية المقاسة للعمليات المتشاكهة والغير متشاكهة مع القيم النظرية والمعلنة لباحثين اخرين ووجد ان النتائج الحالية في توافق مع القيم النظرية.

Introduction

Compton effect is a scattering of gamma or x-ray waves by a charged particle in which a portion of its energy is given to the charged particle in an elastic collision. The major physical effects characterizing the backward-scattered spectra are besides attenuation, Compton shift and material-specific Doppler broadening of the photon spectrum in the sample. The shape of a Compton-broadened peak can reveal information about the electron momentum of an elementary or, even to some extent, of a chemical compound. Essentially, two types of methods were considered for describing the broadening of the characteristic lines. The first calculation procedure evaluated scattered spectra based on tabulated material specific Compton profiles.

The second model was a phenomenological approach; it fitted a function consisting of Gaussian curves above a linearly approximated background to the curvature of the 2nd derivative of the Compton spectrum. These models were experimentally validated on Compton profiles of a variety of sample materials containing period 2 and period 3 elements [1].

It was proven that, in principle, a comparing of measured with calculated spectra provides high material differentiation capabilities, but for most molecules tabulated Compton profiles are not available and the independent atom approximation causes deviations. The phenomenological method was employed to extract Gaussian curve fit-parameters to distinguish measured materials quantitatively. Most of the samples could be distinguished from each other based on their profile structure.

Compton energy absorption cross sections are calculated using the formulas based on a relativistic impulse approximation to assess the contribution of Doppler broadening and to examine the Compton profile literature and explore what, if any, effect our knowledge of this line broadening has on the Compton component in terms of mass–energy absorption coefficient. The electron momentum prior to the scattering event should cause a Doppler broadening of the Compton line [1]. Measurement of differential scattering cross sections for x-rays is useful in the studies of radiation attenuation, transport and energy deposition and plays an important role in medical physics, reactor shielding, industrial radiography in addition to x-ray crystallography. Coherent (Rayleigh) scattering accounts for only a small fraction of the total cross section, contributing to the most of 10% in heavy elements, just below the K-edge energy. Incoherent (Compton) scattering accounts for the rest of the total cross section. For low Z materials, this process dominates over most part of the energy range. The Compton profile-provides detailed information about the electron momentum distribution in the scatterer. The technique is particularly sensitive to the behavior of the slower moving outer electrons involved in bonding in condensed matter and can be used to test their quantum-mechanical description. Mendelsohn, et al., (1974)[2], had made calculations of relativistic Hartree-Fock(HF) Compton profile $J(q)$ for the rare gases and Pb, for values of q between 0 and 100 and compared with the non-relativistic calculations. Comparison with experimental profile data was made for Ar and Kr. For q between 0.0 and 0.4 in Kr, much closer agreement with the experiment was obtained when the relativistic HF wave function was used to perform the profile calculation, when the non-relativistic HF. R Benesch (1976) [3], calculated Compton profile by HF wave functions for the neutral atoms As (Z = 33) to Yb (Z = 70) were the comparison of the results with relativistic HF wave functions indicates that the overall effect of using the relativistic functions is to produce the total $J(q)$, which are flatter at the center than those computed from non-relativistic HF wave functions. Rao et al., (2002) [4], had been calculated the Compton energy absorption cross sections using the formulas based on a relativistic impulse approximation to assess the contribution of Doppler broadening and examine the Compton profile. Using these cross sections, the Compton component of the mass–energy absorption coefficient is derived in the energy region from 1 keV to 1 MeV for all elements with

Z=51 – 100. Also the Compton broadening was estimated using the non-relativistic formula in the angular region 1°–180°, for 17.44, 22.1, 58.83, and 60 keV photons for few elements H, C, N, O, P, S, K, and Ca. Rao et al., (2004) [5], had been used the relativistic and non-relativistic Compton profile cross sections for H, C, N, O, P, and Ca for a few important biological materials such as water, polyethylene, lucite, polystyrene, nylon, polycarbonate, bakelite, fat, bone and calcium hydroxyapatite that estimated for a number of, K, x-ray energies for 59.54 keV (^{241}Am) photons. These values are estimated around the centroid of the Compton profile with an energy interval of 0.1 and 1.0 keV for 59.54 keV photons. Prem Singh (2011) [6], had been studied the Compton scattering differential cross-sections for the 19.648 keV photons in a few elements with ($6 \leq Z \leq 50$).The measured Compton scattering cross-sections were compared with the theoretical Klein-Nishina cross-sections corrected for the non-relativistic HF incoherent scattering function S(X, Z). Hossain, et al., (2012)[7], had been studied Compton scattering using NaI (TI) scintillator detector and a collimated ^{137}Cs source producing gamma rays with an energy of 662 keV scattered incoherently by Al and Cu materials through the angles from (0 to 120°). The Compton scattering effect was investigated and found that the energy of the scattered gamma ray decreases as the scattering angle increases. The differential scattering cross-section as a function of scattering angles was also measured. The experimental results of differential scattering cross-sections for Al and Cu materials were compared with a function of a scattering angle and found to coincide at the higher angle region, although scattering cross-sections for Cu are larger than Al scatter at the lower angles region. In the present work, a proposal for calculating Compton profile required for the calculations of Doppler broadening and Double differential cross section is presented and tested. Different elements and materials are used and tested in this work together with the NaI(Tl) measurement and analysing system. The Compton profile can be determined from measurements of the partial differential cross section by performing a constant energy scan through all possible scattering angle at the scattering angle (180°).

Theory

The differential cross section for the scattering of gamma photons with free electrons was first derived in 1928 by Oskar Klein and Yoshio Nishina [8] using the quantum electrodynamics approach. The angular distribution of the scattered photon is known as the Klein-Nishina cross-section formula and can be given by [9]:

$$\frac{d\sigma}{d\Omega} = \frac{Zr_{\circ}^2}{2}\left(\frac{1+cos^2\theta}{\left(1+\alpha(1-cos\theta)\right)^2}\right)\left(1+\frac{\alpha^2(1-cos\theta)^2}{(1+cos^2\theta)[1+\alpha(1-cos\theta)]}\right) \quad (1)$$

where $\alpha = \frac{E_\gamma}{mc^2}$ and $r_{\circ}$ is the classical electron radius and $\theta = 180°$.

However, what has been stated earlier is valid assuming that the gamma interacts with an electron at rest. But this is an approximation. If the electron momentum is taken into account, neither the angle-energy relations nor the Klein-Nishina formula, Eq. (1) are completely valid. The electron pre-collision momentum creates a broadening in the energy spectrum of the scattered photon which is known as the Doppler broadening effect[10]. The distance travelled by the electron ejected from the atom is shorter than the spatial resolution of today's solid state detectors, which

make it impossible to measure the energy and momentum of the electron in order to correct this effect. This effectively introduces an error on the calculated Compton scattering angle θ.

The angular Klein-Nishina is integrated to give the total cross section for a given energy which is given as [11]:

$$\sigma_{KN} = 2\pi r_{\circ}^2 \left\{\frac{1+\alpha}{\alpha^2}\left[\frac{2(1+\alpha)}{1+2\alpha} - \frac{1}{\alpha}\ln(1+2\alpha)\right] + \frac{1}{2\alpha}\ln(1+2\alpha) - \frac{1+3\alpha}{(1+2\alpha)^2}\right\} \quad (2)$$

The Doppler broadening effect imposes an inherent limitation on the angular resolution. In general the interaction takes place with a bound, moving electron. The momentum of the electron results in a broadening of the gamma spectrum lines and this leads to an error on the computation of the Compton scattering angle. The equation that accounts for the electron movement is [12]

where p_z is the electron momentum,E_γ is the Compton energy calculated from θ (through Eq.3) before the interaction, projected upon the gamma momentum transfer vector. This equation reduces exactly to Eq. (3) taking p_z= 0. The angular distribution is also affected by the electron motion and the Klein-Nishina cross-section must be modified giving the following expression [13]:

$$P_z = -mc\frac{E_\gamma + E_\gamma^{'} - E_\gamma E_\gamma^{'}\frac{1-cos\theta}{mc^2}}{\sqrt{(E_\gamma)^2+(E_\gamma^{'})^2 - 2\,E_\gamma E_\gamma^{'}\,cos\theta}} \quad (3)$$

$$\frac{d^2\sigma}{d\Omega dE_\gamma^{'}} = \frac{mr_{\circ}^2}{2E_\gamma}\left(\frac{E^{'}}{E_\gamma} + \frac{E_\gamma}{E^{'}} - sin^2\theta\right)\frac{E_\gamma^{'}}{\sqrt{(E_\gamma)^2+(E_\gamma^{'})^2 - 2\,E_\gamma E_\gamma^{'}\,cos\theta}}J(p_z) \quad (4)$$

where *J(p_z)*, known as Compton profile which is the electron momentum distribution on the material. The values of Compton profiles are important as they give insight of the electron movement in the atom. They have been calculated using the HF method [13, 14]. DuMond (1933) [15] likened the Doppler-broadening process to the reflection of light from a moving mirror (the electron) with the addition of a wavelength shift fixed by the scattering angle. *J(p_z)* and *J(p_z)*mag. are properties of the scattering electrons. These are the Compton and magnetic Compton profiles. They are defined as the one-dimensional projections of the electron and spin momentum density distributions, respectively. By including the normalizing pre factors 1/N and 1/μ, where N and μ represent the total number of electrons and the spin-unpaired electrons only, we choose the integrated profile areas to be equal to the total charge and spin of the system. Thus,

$$J(pz) = \frac{1}{N}\iint_{-\infty}^{\infty} n(p)dp_x dp_y \quad (5)$$

In an isotropic system the expression is commonly rewritten in terms of the radial momentum distribution *I (p)* = $4\pi p^2 n(p)$ and a scalar momentum variable, *q,* as

$$J(p_z)mag = \frac{1}{\mu}\iint_{-\infty}^{\infty}(n\uparrow(p) - n\downarrow(p))dp_x dp_y \quad (6)$$

where n(p), n↑ (p) and n↓ (p) are the three-dimensional electron momentum distributions for all, majority-spin (↑)

and minority-spin (↓) electrons, respectively. The Compton profile is therefore one dimensional projection of the nuclear momentum distribution along the direction of q. The Compton profile can be determined from measurements of the partial differential cross section by performing a constant energy scan through all possible scattering angles.

Apparatus

The gamma detector used in this work was ("3×3") inch NaI (Tl) scintillation detector. The system is portable and can be used for laboratories and field work. It has a fully-integrated multi-channel analyzer (MCA) tube base that contains a high-voltage power supply and pre amplifier; all supplied by Canberra Industries USA. The source was cylindrical ^{137}Cs, 0.8 cm in the diameter whose activity was 8 mCi giving collimated gamma rays at the exit of the lead collimator of the same dimension. Sample are located 15 cm after the radioactive source and the measurement time was 15 minutes. The experimental, arrangement of the measurements is shown Schematically in Fig. 1.

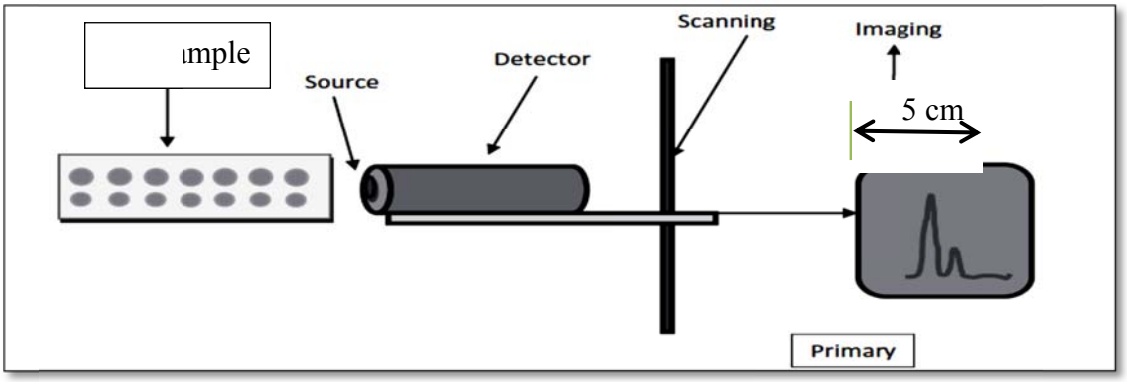

Fig.1: Setup for plate imaging with the source in direct contact with the detector and depressions toward the source.

Results and discussion

The Compton profile was calculated theoretically by equalizing the program table curve, 2D software, version 5.01program. The best estimated theoretical equation is given by

$$J^{-1} = A + B\,Q^{1.5} \qquad (7)$$

where J (Compton profile) and Q (average electron momentum in the ground state of hydrogen).The predicted A and B coefficient is an archived from fitting to the experimental result and theoretical calculation of the Compton profile (J and Q), where the best –fit linear regression line is curved atr^2 =1.

When the parameters (A and B) for these test power intensities are calculated for J and Q value

$A = 0.5775\ Z^{-0.402}$, $B = 7.4473\ Z^{-1.238}$ (8)

In the present work, different elements are taken to measure and calculate the non-relativistic and relativistic double differential scattering cross sections for single atoms such as, Fe, Zn, Ag, Au and Hg. The Compton profile and the double-differential scattering cross section of Doppler broadening as it has been the Compton profile. Are investigated experimentally and the relevant empirical formula is achieved. The results are compared with the theoretical work of references [15] which gives the confidence of the

variation for the present empirical formula for the comparison with other. The Compton profiles *J(Q)* are calculated theoretically using the HF wave functions which are used for the Compton profile on the computations of x-ray cross sections and attenuation coefficients. This is derived on the basis of data that have been explored fully in the literature [8-9]. Furthermore, the behavior of the Compton energy absorption cross sections by means of double differential scattering cross sections based on impulse approximation with the inclusion of Doppler broadening, are shown in Tables 1-5, respectively which are given more attention when the component then with practical results. The difference in sketches between the theoretically convoluted Compton profiles and present experimental Compton profile results are presented in Figs. 2-6.

Table 1: Compton profile and double-differential scattering cross section of doppler broadening for (^{26}Fe).

E_0 (keV)	E_A(keV)	E_C(keV)	Q	A	B	J	$\frac{d^2\sigma}{d\Omega dE_A}$	Q Theo [15]	J Theo [15]
17.44	16.5378	0.902205	0.066339	0.155859	0.131829	6.32464	7.60446E-49	0	6.76E+00
22.1	20.67099	1.429007	0.105074	0.155859	0.131829	6.236382	7.57997E-49	0.05	6.76E+00
23.1	21.5433	1.556701	0.114463	0.155859	0.131829	6.212551	7.56884E-49	0.1	6.55E+00
24.1	22.41053	1.689468	0.124226	0.155859	0.131829	6.18692	7.55553E-49	0.15	6.30E+00
24.2	22.49698	1.703023	0.125222	0.155859	0.131829	6.184257	7.55407E-49	0.2	6.01E+00
25.2	23.35868	1.841322	0.135391	0.155859	0.131829	6.156621	7.53828E-49	0.3	5.36E+00
30.85	28.13493	2.715075	0.199638	0.155859	0.131829	5.965931	7.40558E-49	0.4	4.79E+00
32.06	29.13785	2.922146	0.214864	0.155859	0.131829	5.917544	7.36744E-49	0.5	4.38E+00
33.36	30.20772	3.152281	0.231785	0.155859	0.131829	5.862688	7.32268E-49	0.6	4.11E+00
34.57	31.19646	3.373538	0.248054	0.155859	0.131829	5.809025	7.27753E-49	0.7	3.94E+00
35.86	32.24316	3.616836	0.265944	0.155859	0.131829	5.749136	7.22578E-49	0.8	3.83E+00
39.91	35.48052	4.429479	0.325697	0.155859	0.131829	5.544375	7.04009E-49	1	3.66E+00
42.76	37.71529	5.044708	0.370934	0.155859	0.131829	5.386727	6.88994E-49	1.2	3.49E+00
45.72	39.99941	5.720589	0.420632	0.155859	0.131829	5.213141	6.71905E-49	1.4	3.29E+00
48.72	42.27695	6.443054	0.473754	0.155859	0.131829	5.029002	6.53255E-49	1.6	3.06E+00
48.81	42.3447	6.465301	0.47539	0.155859	0.131829	5.023373	6.52677E-49	1.8	2.82E+00
52.02	44.73977	7.280228	0.535311	0.155859	0.131829	4.819476	6.31487E-49	2	2.58E+00
58.83	49.6864	9.143601	0.672324	0.155859	0.131829	4.375732	5.83818E-49	2.4	2.12E+00
59.54	50.1919	9.3481	0.68736	0.155859	0.131829	4.329288	5.78722E-49	3	1.56E+00
66.24	54.87053	11.36947	0.835991	0.155859	0.131829	3.896735	5.30404E-49	4	9.81E-01
68.18	56.19506	11.98494	0.881246	0.155859	0.131829	3.774766	5.1652E-49	5	6.72E-01

Table 2: Compton profile and double-differential cross section of doppler broadening for (^{30}Zn).

E_0(keV)	E_A(keV)	E_C(keV)	Q	a	b	J	$\frac{d^2\sigma}{d\Omega dE_A}$	[15] Q Theo	J Theo[15]
17.44	16.5378	0.902205	0.066339	0.147146	0.110426	6.709921	8.0677E-49	0	6.76E+00
22.1	20.67099	1.429007	0.105074	0.147146	0.110426	6.626582	8.05423E-49	0.05	6.76E+00
23.1	21.5433	1.556701	0.114463	0.147146	0.110426	6.604034	8.04579E-49	0.1	6.55E+00
24.1	22.41053	1.689468	0.124226	0.147146	0.110426	6.579762	8.03527E-49	0.15	6.30E+00
24.2	22.49698	1.703023	0.125222	0.147146	0.110426	6.577239	8.0341E-49	0.2	6.01E+00
25.2	23.35868	1.841322	0.135391	0.147146	0.110426	6.551042	8.02122E-49	0.3	5.36E+00
30.85	28.13493	2.715075	0.199638	0.147146	0.110426	6.369578	7.90663E-49	0.4	4.79E+00
32.06	29.13785	2.922146	0.214864	0.147146	0.110426	6.323337	7.87266E-49	0.5	4.38E+00
33.36	30.20772	3.152281	0.231785	0.147146	0.110426	6.270818	7.83244E-49	0.6	4.11E+00
34.57	31.19646	3.373538	0.248054	0.147146	0.110426	6.219342	7.79158E-49	0.7	3.94E+00
35.86	32.24316	3.616836	0.265944	0.147146	0.110426	6.161778	7.74441E-49	0.8	3.83E+00
39.91	35.48052	4.429479	0.325697	0.147146	0.110426	5.964036	7.57297E-49	1	3.66E+00
42.76	37.71529	5.044708	0.370934	0.147146	0.110426	5.810804	7.43236E-49	1.2	3.49E+00
45.72	39.99941	5.720589	0.420632	0.147146	0.110426	5.641078	7.2706E-49	1.4	3.29E+00
48.72	42.27695	6.443054	0.473754	0.147146	0.110426	5.459873	7.09224E-49	1.6	3.06E+00
48.81	42.3447	6.465301	0.47539	0.147146	0.110426	5.454314	7.08669E-49	1.8	2.82E+00
52.02	44.73977	7.280228	0.535311	0.147146	0.110426	5.252218	6.88188E-49	2	2.58E+00
58.83	49.6864	9.143601	0.672324	0.147146	0.110426	4.807199	6.41385E-49	2.4	2.12E+00
59.54	50.1919	9.3481	0.68736	0.147146	0.110426	4.760206	6.36325E-49	3	1.56E+00
66.24	54.87053	11.36947	0.835991	0.147146	0.110426	4.318677	5.87837E-49	4	9.81E-01
68.18	56.19506	11.98494	0.881246	0.147146	0.110426	4.192905	5.73736E-49	5	6.72E-01

Table 3: Compton profile and double-differential cross section of doppler broadening for (^{47}Ag).

E_0(keV)	E_A(keV)	E_C(keV)	Q	a	b	J	$\frac{d^2\sigma}{d\Omega dE_A}$	Q Theo[15]	J Theo[15]
17.44	16.5378	0.902205	0.066339	0.122848	0.063342	8.069043	9.70185E-49	0	8.81E+00
22.1	20.67099	1.429007	0.105074	0.122848	0.063342	7.999643	9.72311E-49	0.05	8.13E+00
23.1	21.5433	1.556701	0.114463	0.122848	0.063342	7.980775	9.7231E-49	0.1	8.01E+00
24.1	22.41053	1.689468	0.124226	0.122848	0.063342	7.960419	9.72134E-49	0.15	7.82E+00
24.2	22.49698	1.703023	0.125222	0.122848	0.063342	7.9583	9.72106E-49	0.2	7.59E+00
25.2	23.35868	1.841322	0.135391	0.122848	0.063342	7.936273	9.71732E-49	0.3	7.14E+00
30.85	28.13493	2.715075	0.199638	0.122848	0.063342	7.782207	9.66014E-49	0.4	6.79E+00
32.06	29.13785	2.922146	0.214864	0.122848	0.063342	7.742527	9.63957E-49	0.5	6.54E+00
33.36	30.20772	3.152281	0.231785	0.122848	0.063342	7.69725	9.6141E-49	0.6	6.73E+00
34.57	31.19646	3.373538	0.248054	0.122848	0.063342	7.652653	9.58722E-49	0.7	6.22E+00
35.86	32.24316	3.616836	0.265944	0.122848	0.063342	7.602523	9.5552E-49	0.8	6.07E+00
39.91	35.48052	4.429479	0.325697	0.122848	0.063342	7.428217	9.43214E-49	1	5.70E+00
42.76	37.71529	5.044708	0.370934	0.122848	0.063342	7.290859	9.32544E-49	1.2	5.24E+00
45.72	39.99941	5.720589	0.420632	0.122848	0.063342	7.136325	9.19778E-49	1.4	4.75E+00
48.72	42.27695	6.443054	0.473754	0.122848	0.063342	6.968499	9.05191E-49	1.6	4.24E+00
48.81	42.3447	6.465301	0.47539	0.122848	0.063342	6.963304	9.04729E-49	1.8	3.77E+00
52.02	44.73977	7.280228	0.535311	0.122848	0.063342	6.772469	8.87384E-49	2	3.35E+00
58.83	49.6864	9.143601	0.672324	0.122848	0.063342	6.338466	8.45689E-49	2.4	2.67E+00
59.54	50.1919	9.3481	0.68736	0.122848	0.063342	6.29149	8.41021E-49	3	2.02E+00
66.24	54.87053	11.36947	0.835991	0.122848	0.063342	5.838918	7.94765E-49	4	1.50E+00
68.18	56.19506	11.98494	0.881246	0.122848	0.063342	5.706174	7.80804E-49	5	1.12E+00

Table 4: Compton profile and double-differential scattering cross section of doppler broadening for (^{79}Au).

E_0(keV)	E_A(keV)	E_C(keV)	Q	a	b	J	$\frac{d^2\sigma}{d\Omega dE_A}$	Q Theo[15]	J Theo[15]
17.44	16.5378	0.902205	0.066339	0.099702	0.033303	9.972924	1.1991E-48	0	1.00E+01
22.1	20.67099	1.429007	0.105074	0.099702	0.033303	9.917018	1.2054E-48	0.05	9.99E+00
23.1	21.5433	1.556701	0.114463	0.099702	0.033303	9.901759	1.2063E-48	0.1	9.90E+00
24.1	22.41053	1.689468	0.124226	0.099702	0.033303	9.88527	1.2072E-48	0.15	9.78E+00
24.2	22.49698	1.703023	0.125222	0.099702	0.033303	9.883552	1.2073E-48	0.2	9.61E+00
25.2	23.35868	1.841322	0.135391	0.099702	0.033303	9.865673	1.208E-48	0.3	9.25E+00
30.85	28.13493	2.715075	0.199638	0.099702	0.033303	9.739649	1.209E-48	0.4	8.92E+00
32.06	29.13785	2.922146	0.214864	0.099702	0.033303	9.706914	1.2085E-48	0.5	8.66E+00
33.36	30.20772	3.152281	0.231785	0.099702	0.033303	9.669422	1.2077E-48	0.6	8.45E+00
34.57	31.19646	3.373538	0.248054	0.099702	0.033303	9.632347	1.2067E-48	0.7	8.25E+00
35.86	32.24316	3.616836	0.265944	0.099702	0.033303	9.590497	1.2054E-48	0.8	8.05E+00
39.91	35.48052	4.429479	0.325697	0.099702	0.033303	9.443523	1.1991E-48	1	7.57E+00
42.76	37.71529	5.044708	0.370934	0.099702	0.033303	9.326082	1.1929E-48	1.2	7.0OE+00
45.72	39.99941	5.720589	0.420632	0.099702	0.033303	9.192212	1.1848E-48	1.4	6.40E+00
48.72	42.27695	6.443054	0.473754	0.099702	0.033303	9.044691	1.1749E-48	1.6	5.81E+00
48.81	42.3447	6.465301	0.47539	0.099702	0.033303	9.040088	1.1746E-48	1.8	5.27E+00
52.02	44.73977	7.280228	0.535311	0.099702	0.033303	8.869495	1.1622E-48	2	4.80E+00
58.83	49.6864	9.143601	0.672324	0.099702	0.033303	8.470152	1.1301E-48	2.4	4.08E+00
59.54	50.1919	9.3481	0.68736	0.099702	0.033303	8.42595	1.1263E-48	3	3.44E+00
66.24	54.87053	11.36947	0.835991	0.099702	0.033303	7.98988	1.0875E-48	4	2.85E+00
68.18	56.19506	11.98494	0.881246	0.099702	0.033303	7.858356	1.0753E-48	5	2.36E+00

Table 5: Compton profile and double-differential scattering cross section of doppler broadening for (^{80}Hg).

E_0(keV)	E_A(keV)	E_C(keV)	Q	a	b	J	$\frac{d^2\sigma}{d\Omega dE_A}$	Q Theo[15]	J Theo[15]
17.44	16.5378	0.902205	0.066339	0.0992	0.032789	10.02408	1.20525E-48	0	1 .08E+01
22.1	20.67099	1.429007	0.105074	0.0992	0.032789	9.968465	1.21161E-48	0.05	1 .08E+01
23.1	21.5433	1.556701	0.114463	0.0992	0.032789	9.953286	1.21262E-48	0.1	1.06E+01
24.1	22.41053	1.689468	0.124226	0.0992	0.032789	9.936881	1.2135E-48	0.15	1.04E+01
24.2	22.49698	1.703023	0.125222	0.0992	0.032789	9.935172	1.21358E-48	0.2	1.02E+01
25.2	23.35868	1.841322	0.135391	0.0992	0.032789	9.917385	1.2143E-48	0.3	9.57E+00
30.85	28.13493	2.715075	0.199638	0.0992	0.032789	9.791987	1.21549E-48	0.4	9.02E+00
32.06	29.13785	2.922146	0.214864	0.0992	0.032789	9.75941	1.21506E-48	0.5	8.60E+00
33.36	30.20772	3.152281	0.231785	0.0992	0.032789	9.722095	1.21432E-48	0.6	8.21E+00
34.57	31.19646	3.373538	0.248054	0.0992	0.032789	9.685193	1.21336E-48	0.7	8.05E+00
35.86	32.24316	3.616836	0.265944	0.0992	0.032789	9.643535	1.21204E-48	0.8	7.85E+00
39.91	35.48052	4.429479	0.325697	0.0992	0.032789	9.497204	1.20593E-48	1	7.45E+00
42.76	37.71529	5.044708	0.370934	0.0992	0.032789	9.380245	1.19979E-48	1.2	6.97E+00
45.72	39.99941	5.720589	0.420632	0.0992	0.032789	9.24689	1.1918E-48	1.4	6.43E+00
48.72	42.27695	6.443054	0.473754	0.0992	0.032789	9.099893	1.18205E-48	1.6	5.88E+00
48.81	42.3447	6.465301	0.47539	0.0992	0.032789	9.095306	1.18174E-48	1.8	5.35E+00
52.02	44.73977	7.280228	0.535311	0.0992	0.032789	8.92526	1.16946E-48	2	4.88E+00
58.83	49.6864	9.143601	0.672324	0.0992	0.032789	8.526962	1.13768E-48	2.4	4.14E+00
59.54	50.1919	9.3481	0.68736	0.0992	0.032789	8.482855	1.13395E-48	3	3.45E+00
66.24	54.87053	11.36947	0.835991	0.0992	0.032789	8.047506	1.09539E-48	4	2.85E+00
68.18	56.19506	11.98494	0.881246	0.0992	0.032789	7.916122	1.0832E-48	5	2.38E+00

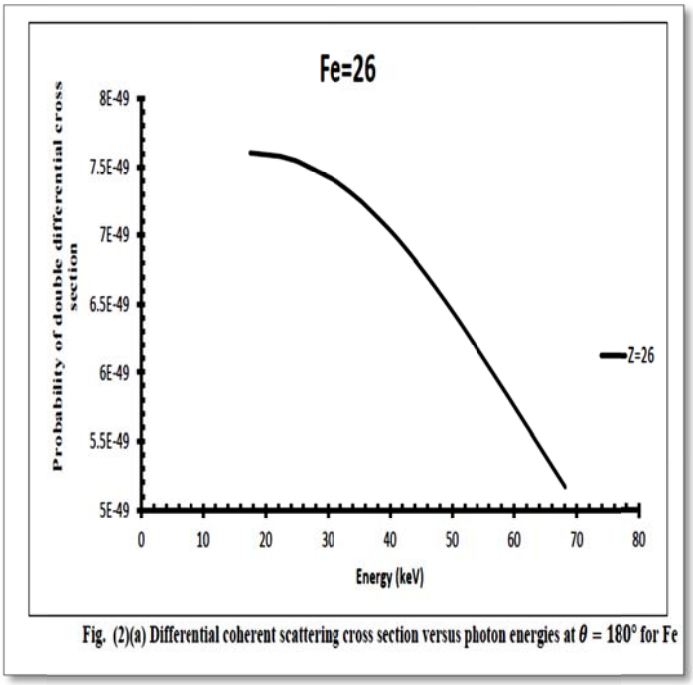

Fig. (2)(a) Differential coherent scattering cross section versus photon energies at $\theta = 180°$ for Fe

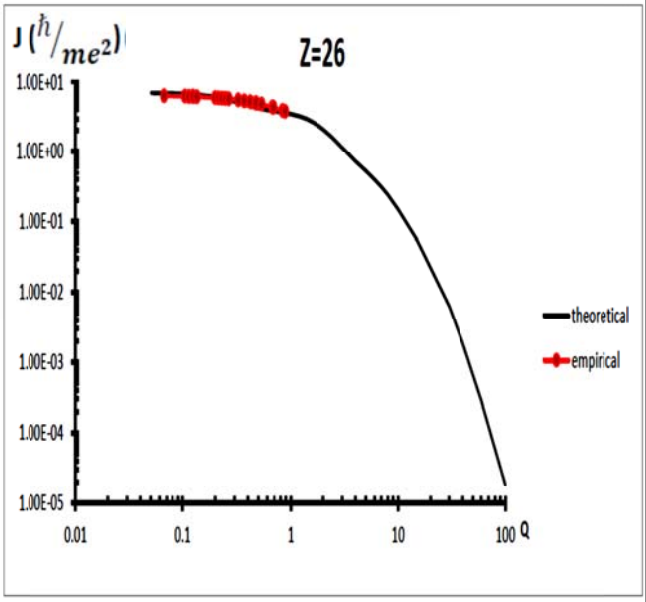

Fig. (2)(b)Comparison of the theoretical & empirical values for Compton profile

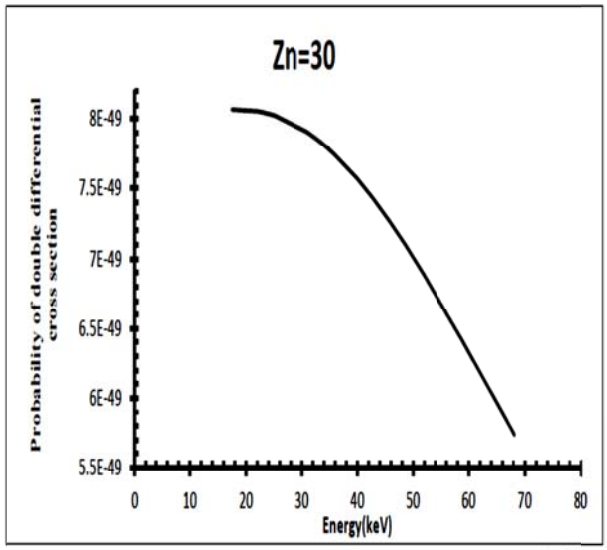

Fig. (3)(a) Differential coherent scattering cross section versus photon energies at $\theta = 180°$ for Zn

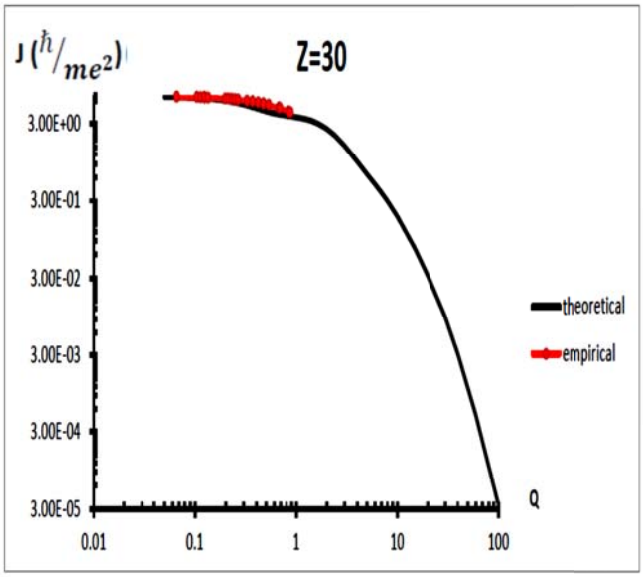

Fig. (3)(b)Comparison of the theoretical & empirical values for Compton profile

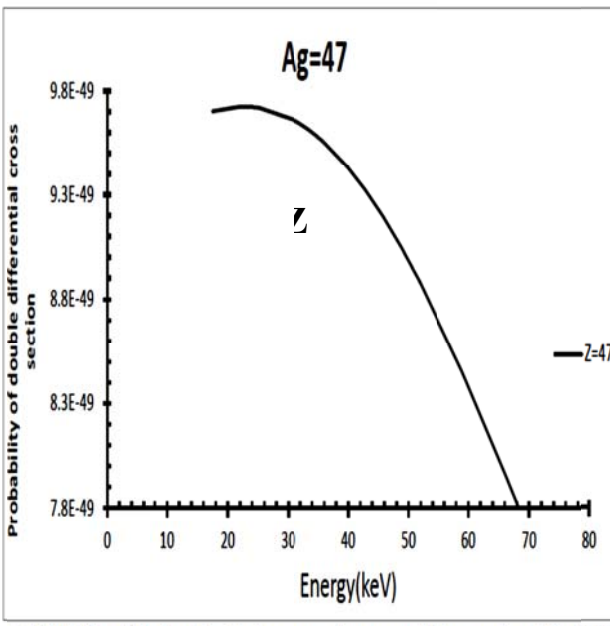

Fig. (4)(a) Differential coherent scattering cross section versus photon energies at $\theta = 180°$ for Ag

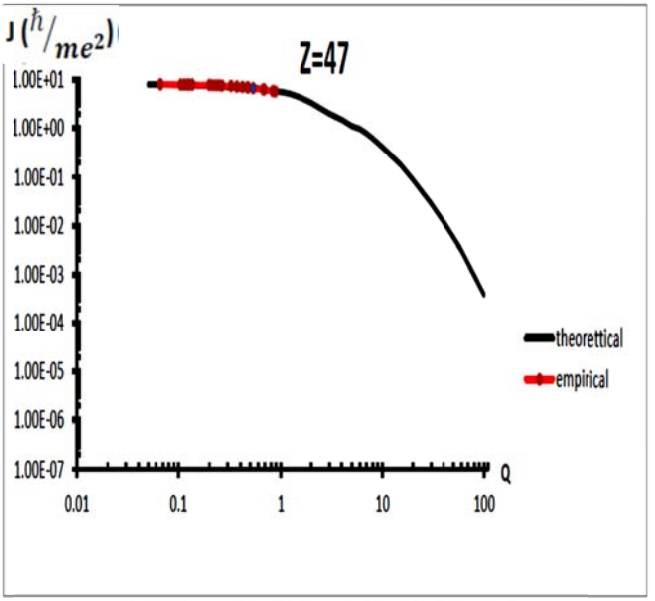

Fig. (4)(b)Comparison of the theoretical & empirical values for Compton profile

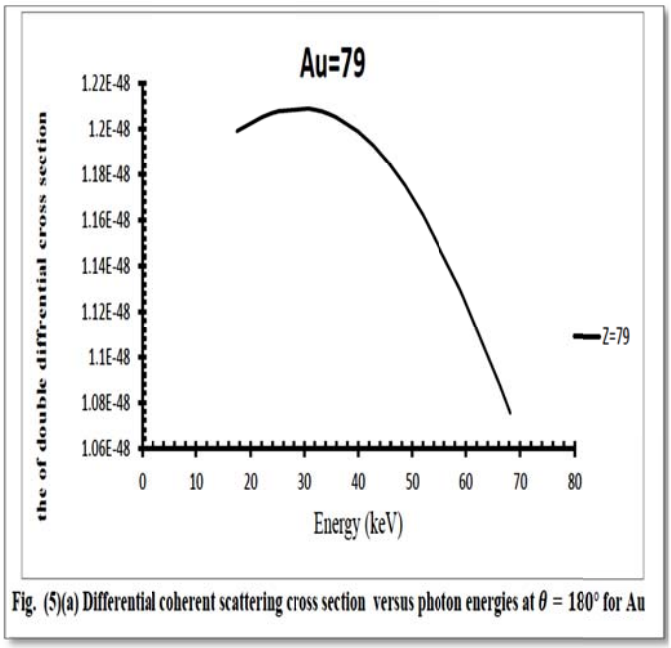

Fig. (5)(a) Differential coherent scattering cross section versus photon energies at $\theta = 180°$ for Au

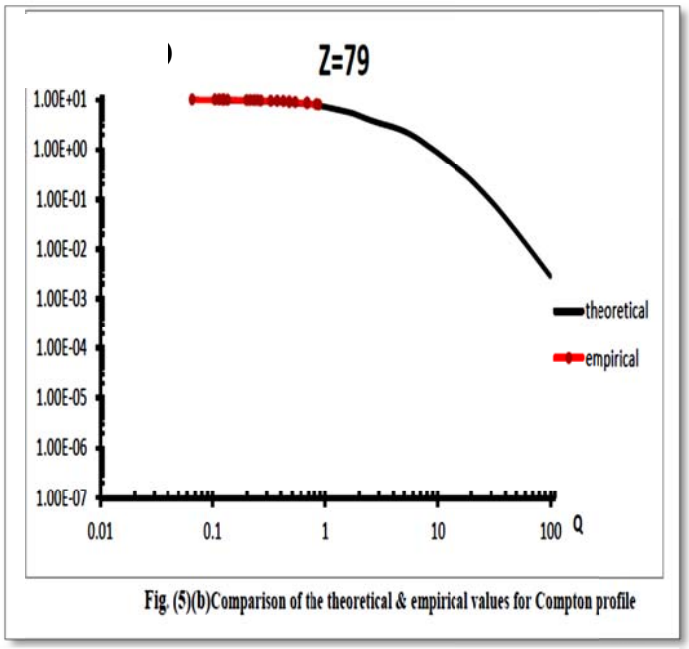

Fig. (5)(b)Comparison of the theoretical & empirical values for Compton profile

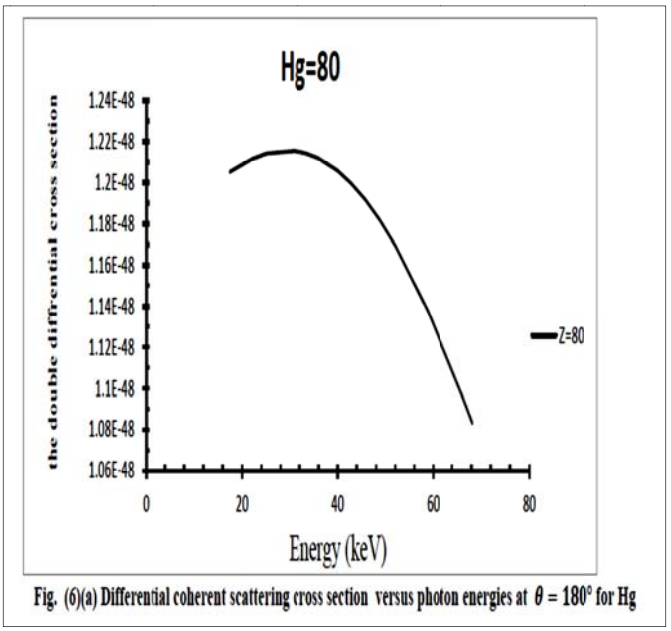

Fig. (6)(a) Differential coherent scattering cross section versus photon energies at $\theta = 180°$ for Hg

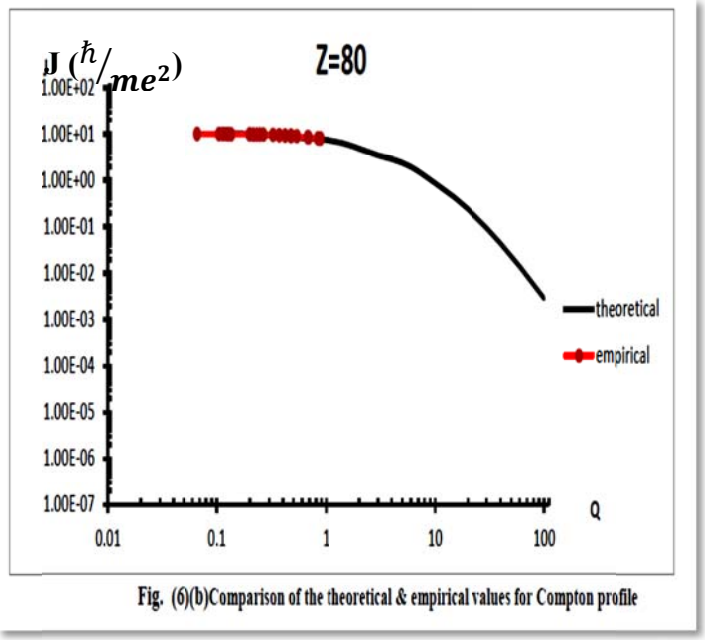

Fig. (6)(b)Comparison of the theoretical & empirical values for Compton profile

From the comparisons shown in Tables 1-5 and Figs.(2b)-(6b),the behavior of the predicted experimental results using Eqs. (1-3) and (1-4) is found in consistency with theoretical calculations [15].

Form these comparisons we found a necessity of calculation for extending theoretical total Compton profile for the free atom is needed., As shown before the Doppler broadening is due to bound-electron Compton scattering, which is a significant source of energy uncertainty, therefore this limits the choice of scattering detectors to low-Z materials, where the Doppler broadening is less and the relative probability of Compton scattering is higher. Also, these shown the importance of the energy resolution of the absorption detector in the determination of the electronic properties of solids.

Conclusions

1-From surveying the behavior of Compton profile distribution (theoretical and experimental) over a

wide range of element samples, one can observe found the necessity of extending these profiles to include lower energy photon scattering, which is a significant source of energy uncertainty. This limits the choice of scatter detectors to low-Z materials, where the Doppler broadening is less and the relative probability of Compton scattering is higher. Also, We have shown the importance of the energy resolution of the absorption detector.

2-The Compton profile data are useful to assess the contribution of Doppler broadening and to calculate the Compton component of the mass energy absorption coefficient.

3-The effect of Compton broadening is significant at energies below 100 keV and must be considered, since it spreads the counts in the neighboring isogonic regions.

References

[1] A. H. Compton, Phys. Rev., 21, 5 (1923) 483-502.

[2] L.B. Mendelsohn, Frank Biggs, J. B. Mann, Original Research Article Chem. Phys. Lett. 26 (1974) 521-524.

[3] M. Descovich, P.J. Nolana, A.J. Bostona, J. Dobsona, S. Grosa, J.R. Cresswella, J. Simpsonb, I. Lazarusb, P.H. Reganc, J.J. Valiente-Dobonc, P. Sellinc, C.J. Pearsonc, Nucl. Instr. and Meth. A 553 (2005) 512-521.

[4] D. V. Rao, b. T. Takeda, Y. Itai, T. J. Akatsuka, Phys. Chem. Ref. Data, 31, 3 (2002) 769-818.

[5] D. Rao, V. R. Cesareo, A. Brunetti, J. of Phys. and Chem. Ref. Data, 33 (2004) 627-712.

[6] P.Singh, Nature and Science, 9, 10 (2011) 1545-0740.

[7] I. Hossain, N. A Azmi, M. A. Saeed, M. E. Hoque, K. K. Viswanathan, H. Y. Abdullah, Inter. J. of the Phys. S. 7, 4 (2012) 544-549.

[8] S. Gowda, S. Krishnaveni, T. Yashoda, T. K. Umesh, R. Gowda, J. Phys. 63 (2004) 529-541.

[9] I. Han, L.Demir Nucl. Instrum. Methods, B267 (2009) 3505-3510.

[10] E. do Nascimento, O. Helene, C. Takiya, V.R. Vanin, Doppler broadening of positron annihilation radiation: fitting the coincidence spectrum, Nucl. Instr. and Meth. in Physics Research Section A, 538, Issues 1–3, 11 (2005) 723–730.

[11] J.L. Dobson, Ph.D. Thesis, The characterization and position resolution of a planar germanium strip detector, university of Liverpool, UK, 2005.

[12] C.E. Ordonez, A. Bolozdynya, W. Chang. In Nuclear Science Symposium IEEE, 2 (1997) 1361-1365.

[13] R. Ribberfors, Relationship of the relativistic Compton cross section to the momentum distribution of bound electron states, Phys. Rev. B. 12, (1975) 2067-2074.

[14] Y.F. Du, Z. He, G.F. Knoll, D.K. Wehe, W. Li, Nucl. Instr. and Meth. in Phys. Res., 457 (2001) 203–211.

[15] F. Biggs, L.B. Mendelsohn, J.B. Mann. Atom. Data and Nucl. Data Tables, 16, 3 (1975) 201- 309.